Nonlinear Dyn (2016) 83:2171–2181
DOI 10.1007/s11071-015-2473-7

ORIGINAL PAPER

Adaptive trajectory tracking control approach for a model-scaled helicopter

Yao Zou

Received: 10 June 2015 / Accepted: 24 October 2015 / Published online: 5 November 2015

Abstract This paper investigates an adaptive trajectory tracking control approach for a model-scaled helicopter with rotation matrix describing its attitude kinematics. The helicopter is decomposed into a cascaded form with some unmodeled dynamics, so that a hierarchical strategy is applicable. First, in the outer position loop, based on an integral-quadratic Lyapunov function, a position control law with hyperbolic tangent functions is designed to accomplish the position tracking. Then, a command rotation matrix is extracted with the minimum rotation principle. Finally, in the inner attitude loop, based on a barrier-quadratic Lyapunov function, a singularity-free attitude control law is designed to realize the attitude tracking. In addition, the bounds of the unmodeled dynamics are estimated and compensated with adaptive algorithms. Simulations on a model-scaled helicopter confirm the proposed control approach.

Keywords Adaptive control · Trajectory tracking · Model-scaled helicopter · Rotation matrix

Y. Zou (✉)
The Seventh Research Division, Beihang University, Beijing 100191, China
e-mail: zouyao20@126.com

1 Introduction

In the last decades, helicopters, especially model-scaled ones, have attracted more and more attention. With capacities of vertically taking off and landing, hovering and low-speed flight, they have been widely employed in reconnaissance, surveillance, agriculture and other fields. However, due to their under-actuated nature, complex aerodynamics and strong coupling, there are still difficulties for researches to design high-performance, robust control approaches for helicopters.

Up to now, there are numerous available nonlinear trajectory tracking approaches for VTOL-UAVs, such as backstepping [1,2], nonlinear dynamic inversion [3,4], model predictive control (MPC) [5] and H_∞ [6]. Among them, hierarchical control approach is more commonly used, which is of a two-stage architecture consisting of a "low-level" fast inner loop and a "high-level" slow outer loop [7]. Zuo and Ru [8], Zuo and Ding [9], Cabecinhas et al. [10] adopted the hierarchical control approach to achieve the trajectory tracking for quad-rotors under external disturbances. Abdessameud and Sharifi [11], Abdessameud and Tayebi [12] accomplished the trajectory and target tracking for VTOL-UAVs using the hierarchical control approach without the linear velocity. However, the above control approaches are based on the model with the Euler angle or unit quaternion describing the attitude kinematics. Despite the fact that Euler angle is a minimal representation, it is defined locally and exhibits singu-

larity for aggressive maneuvers [13]. For the quaternion, unwinding phenomenon, where the sign ambiguity leads to unnecessary large-angle rotation, may lead to discontinuity [14]. Instead, the rotation matrix has received much interest [15], in that it is available for a wider scope and capable of avoiding ambiguity and discontinuity.

Compared with other VTOL-UAVs, model-scaled helicopters are of more model uncertainty, which may affect the tracking performance seriously. In [1,2,16], neural network, nonlinear damping and disturbance observer were, respectively, employed to estimate and compensate unmodeled dynamics; however, they have their problems as well. Large number of nodes of the neural network may increase the algorithm complexity [8]; the nonlinear damping may result in a large control input [17]; and the disturbance observer requires large observer parameters [18].

In this paper, an adaptive hierarchical control approach is proposed for the model-scaled helicopter to achieve the trajectory tracking. The attitude kinematics of the helicopter is represented with the rotation matrix proposed in [19]. The position and attitude loop controls are designed separately. In the position loop, based on an integral-quadratic Lyapunov function, a position loop control with hyperbolic tangent functions is designed. As an intermediate step, a command rotation matrix is extracted. In the attitude loop, to avoid singularity proposed in [19], an attitude loop control is designed based on a barrier-quadratic Lyapunov function [20]. The contributions of this paper are as follows:

(i) the minimum rotation principle is used to extract a command attitude, and criteria of control parameters are built to avoid singularity during the extraction;
(ii) with the attitude represented by the rotation matrix, a singularity-free attitude control is developed;
(iii) the upper bounds of the unmodeled dynamics are estimated with adaptive algorithms.

The configuration of this paper is arranged as follows: Sect. 2 provides the problem statements, Sect. 3 presents the main control approach design, Sect. 4 carries out some simulations on a model-scaled helicopter, and Sect. 5 draws conclusions.

2 Problem statements

2.1 Preliminaries

In the following, $\boldsymbol{I_3} \in \mathbb{R}^{3\times 3}$ denotes a 3×3 identity matrix, $\|\cdot\|$ denotes the Euclidean norm of a vector, $\mathrm{tr}(\cdot)$ denotes the trace of a square matrix, $\bar{\lambda}(\cdot)$ and $\underline{\lambda}(\cdot)$ denote the maximum and minimum eigenvalues of a square matrix. For $\boldsymbol{x} = [x_1, x_2, x_3]^T \in \mathbb{R}^3$, superscript $\times$ indicates the transformation from $\boldsymbol{x}$ to a 3×3 skew-symmetric matrix, namely

$$\boldsymbol{x}^{\times} = \begin{bmatrix} 0 & -x_3 & x_2 \\ x_3 & 0 & -x_1 \\ -x_2 & x_1 & 0 \end{bmatrix},$$

and superscript $\vee$ denotes the inverse operation of $\times$. For $x \in \mathbb{R}$, define the hyperbolic tangent function

$$\tanh(x) = \frac{e^x - e^{-x}}{e^x + e^{-x}},$$

which is differential and satisfies $-1 < \tanh(x) < 1$. For $\boldsymbol{x} = [x_1, \ldots, x_n]^T \in \mathbb{R}^n$, define the hyperbolic tangent function vector

$$\mathbf{tanh}(\boldsymbol{x}) = [\tanh(x_1), \ldots, \tanh(x_n)]^T,$$

the hyperbolic tangent function matrix

$$\mathbf{Tanh}(\boldsymbol{x}) = \mathrm{diag}(\tanh(x_1), \ldots, \tanh(x_n)),$$

and the integral function

$$\int_{\mathbf{0}}^{\boldsymbol{x}} \mathbf{tanh}(\chi)\mathrm{d}\chi = \int_0^{x_1} \tanh(\chi)\mathrm{d}\chi + \cdots + \int_0^{x_n} \tanh(\chi) d\chi.$$

Property 1 ([21]) Given an interval $\{\boldsymbol{x} \in \mathbb{R}^n | \|\boldsymbol{x}\| < \bar{x}, \bar{x} > 0\}$, there always exists a constant $\chi(\bar{x})$ satisfying $0 < \chi < 1$, such that $\chi\|\boldsymbol{x}\| \le \|\mathbf{tanh}(\boldsymbol{x})\| \le \|\boldsymbol{x}\|$.

Lemma 1 ([22]) *Given a constant $\epsilon > 0$, the following inequality holds for all $x \in \mathbb{R}$*

$$0 \le |x| - x\tanh\left(\frac{x}{\epsilon}\right) \le k_q\epsilon, \tag{1}$$

where $k_q = 0.2758$.

Lemma 2 ([23]) *The following inequality holds for all $\boldsymbol{x} \in \{\boldsymbol{x} \in \mathbb{R}^n | \|\boldsymbol{x}\| < k, k > 0\}$*

$$\ln\frac{k^2}{k^2 - \|\boldsymbol{x}\|^2} \le \frac{\|\boldsymbol{x}\|^2}{k^2 - \|\boldsymbol{x}\|^2}. \tag{2}$$

2.2 Helicopter model

The helicopter model is established in two frames: the earth frame $\mathcal{E} = \{oxyz\}$ and the body frame $\mathcal{B} = \{o_b x_b y_b z_b\}$, the definitions of which are in accordance with [1]. The frame $\mathcal{E}$ serves as the inertial frame, and the helicopter is regarded as a 6-dof rigid body. According to [1], the helicopter model is

$$\dot{\boldsymbol{p}} = \boldsymbol{v}, \tag{3}$$

$$\dot{\boldsymbol{v}} = -g\boldsymbol{e_3} + \frac{1}{m}\boldsymbol{R}\boldsymbol{f}, \tag{4}$$

$$\dot{\boldsymbol{R}} = \boldsymbol{R}\boldsymbol{\omega}^{\times}, \tag{5}$$

$$\boldsymbol{J}\dot{\boldsymbol{\omega}} = -\boldsymbol{\omega}^{\times}\boldsymbol{J}\boldsymbol{\omega} + \boldsymbol{\tau}, \tag{6}$$

where $\boldsymbol{p} = [p_x, p_y, p_z]^T$ and $\boldsymbol{v} = [v_x, v_y, v_z]^T$ are the position and velocity of the helicopter c.g. (center of gravity) in the frame $\mathcal{E}$, m is the mass, g is the gravitational acceleration, $\boldsymbol{e_3} = [0, 0, 1]^T$, $\boldsymbol{R} \in SO(3) = \{\boldsymbol{R} \in \mathbb{R}^{3\times3} | \det \boldsymbol{R} = 1, \boldsymbol{R}^T\boldsymbol{R} = \boldsymbol{R}\boldsymbol{R}^T = \boldsymbol{I_3}\}$ is the rotation matrix from the frame $\mathcal{B}$ to the frame $\mathcal{E}$, $\boldsymbol{\omega} = [\omega_x, \omega_y, \omega_z]^T$ is the angular velocity of the helicopter in the frame $\mathcal{B}$, and $\boldsymbol{J} = \mathrm{diag}(J_x, J_y, J_z)$ is the inertial matrix.

During the low-speed flight, the applied force $\boldsymbol{f}$ and torque $\boldsymbol{\tau}$ are mainly generated by the main and tail rotors, which, according to [24], are derived as

$$\boldsymbol{f} = \begin{bmatrix} T_m \mathrm{s}a_s \\ -T_m \mathrm{s}b_s + T_t \\ T_m \mathrm{c}b_s \mathrm{c}a_s \end{bmatrix},$$

$$\boldsymbol{\tau} = \begin{bmatrix} T_m h_m \mathrm{s}b_s + L_b b_s + T_t h_t + \tau_m \mathrm{s}a_s \\ T_m l_m + T_m h_m \mathrm{s}a_s + M_a a_s + \tau_t - \tau_m \mathrm{s}b_s \\ -T_m l_m \mathrm{s}b_s - T_t l_t + \tau_m \mathrm{c}a_s \mathrm{c}b_s \end{bmatrix},$$

where $\mathrm{c}(\cdot) = \cos(\cdot)$, $\mathrm{s}(\cdot) = \sin(\cdot)$, subscripts m and t denote the main and tail rotors, T_i and τ_i ($i = m$ or t) are the thrust and anti-torque generated by the main or tail rotor, L_b and M_a are the stiffness coefficients of the main rotor, h_i and l_i ($i = m$ or t) are the horizontal and vertical positions of the main or tail rotor with respect to the helicopter c.g., a_s and b_s are the longitudinal and lateral flapping angles of the main rotor. Further, τ_i ($i = m$ or t) can be determined by

$$\tau_i = C_i |T_i|^{1.5} + D_i, \tag{7}$$

where C_i and D_i are the aerodynamic constants.

2.3 Helicopter model for control approach design

In view of strong coupling, it is necessary to decompose the applied force and torque for ease of the control approach design. Specifically, according to [25], the flapping angles are fairly small, so that the small angle approximation is feasible, namely $\cos(\cdot) \approx 1$ and $\sin(\cdot) \approx (\cdot)$; moveover, $T_m a_s$, $T_m b_s$ and T_t contribute little to the applied force $\boldsymbol{f}$ and τ_t exerts little to the applied torque $\boldsymbol{\tau}$. Thus, we can decompose $\boldsymbol{f}$ and $\boldsymbol{\tau}$ as

$$\boldsymbol{f} = T_m\boldsymbol{e_3} + \boldsymbol{f_\Delta}, \tag{8}$$

$$\boldsymbol{\tau} = \boldsymbol{\tau_c} + \boldsymbol{\Delta_\tau} = \boldsymbol{\tau_A}\boldsymbol{M} + \boldsymbol{\tau_B} + \boldsymbol{\Delta_\tau}, \tag{9}$$

where

$$\boldsymbol{\tau_A} = \begin{bmatrix} h_t & \tau_m & T_m h_m + L_b \\ 0 & T_m h_m + M_a & -\tau_m \\ -l_t & 0 & -T_m l_m \end{bmatrix},$$

$$\boldsymbol{M} = \begin{bmatrix} T_t \\ a_s \\ b_s \end{bmatrix}, \quad \boldsymbol{\tau_B} = \begin{bmatrix} 0 \\ T_m l_m \\ \tau_m \end{bmatrix},$$

$$\boldsymbol{f_\Delta} = \begin{bmatrix} T_m \mathrm{s}a_s \\ -T_m \mathrm{s}b_s + T_t \\ T_m(\mathrm{c}a_s \mathrm{c}b_s - 1) \end{bmatrix},$$

$$\boldsymbol{\Delta_\tau} = \begin{bmatrix} \tau_m(\mathrm{s}a_s - a_s) + T_m h_m(\mathrm{s}b_s - b_s) \\ \tau_t - \tau_m(\mathrm{s}b_s - b_s) + T_m h_m(\mathrm{s}a_s - a_s) \\ \tau_m(\mathrm{c}a_s \mathrm{c}b_s - 1) - T_m l_m(\mathrm{s}b_s - b_s) \end{bmatrix}.$$

Substituting (8) into (4) and (9) into (6) yields

$$\dot{\boldsymbol{v}} = -g\boldsymbol{e_3} + \frac{T_m}{m}\boldsymbol{R}\boldsymbol{e_3} + \boldsymbol{\Delta}_f, \tag{10}$$

$$\boldsymbol{J}\dot{\boldsymbol{\omega}} = -\boldsymbol{\omega}^{\times}\boldsymbol{J}\boldsymbol{\omega} + \boldsymbol{\tau_c} + \boldsymbol{\Delta_\tau}, \tag{11}$$

where $\boldsymbol{\Delta}_f = \frac{1}{m}\boldsymbol{R}^T\boldsymbol{f_\Delta}$.

Assumption 1 $\boldsymbol{\Delta_\tau}$ and $\boldsymbol{\Delta}_f$ are bounded and satisfy

$$|\Delta_{fi}| \le \sigma_i, \ |\Delta_{\tau i}| \le \varsigma_i, \quad i = 1, 2, 3, \tag{12}$$

where $\boldsymbol{\sigma} = [\sigma_1, \sigma_2, \sigma_3]^T$ and $\boldsymbol{\varsigma} = [\varsigma_1, \varsigma_2, \varsigma_3]^T$ are two unknown upper bound vectors.

Remark 1 Assumption 1 is reasonable, since the unmodeled dynamics $\boldsymbol{\Delta}_f$ and $\boldsymbol{\Delta_\tau}$, usually restricted by physical properties of a typical helicopter, are extremely small [1]. In [26,27], they are disregarded

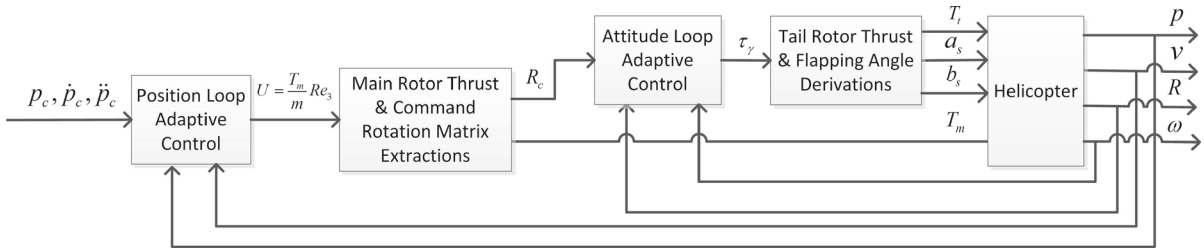

Fig. 1 Block diagram of the proposed control approach

directly. In this paper, we will estimate and compensate their upper bounds to improve the tracking performance.

3 Control approach design

Given a smooth reference trajectory $\boldsymbol{p_c} = [p_{cx}, p_{cy}, p_{cz}]^T$ with its derivatives $\dot{\boldsymbol{p}}_{\boldsymbol{c}}$ and $\ddot{\boldsymbol{p}}_{\boldsymbol{c}}$, the control objective is to design control inputs T_m, T_t, a_s and b_s for the model-scaled helicopter, so that it can track $\boldsymbol{p_c}$. Since the decomposed helicopter model is in a cascade structure, a hierarchical strategy is adopted, so that the position and attitude loop controls are designed separately. The block diagram of the control scheme is displayed in Fig. 1. First, in the position loop, $\frac{T_m}{m}\boldsymbol{Re_3}$ is designed to achieve the position tracking to $\boldsymbol{p_c}$. Then, the main rotor thrust T_m and the command rotation matrix $\boldsymbol{R_c}$ are derived from $\frac{T_m}{m}\boldsymbol{Re_3}$; this step is the common denominator of hierarchical nonlinear controllers [7]. Finally, in the attitude loop, T_t, a_s and b_s are designed to realize the attitude tracking to $\boldsymbol{R_c}$.

3.1 Position loop control design

For ease of analysis, denote $\boldsymbol{U} = [U_x, U_y, U_z]^T = \frac{T_m}{m}\boldsymbol{Re_3}$. Define the position and velocity tracking errors as $\boldsymbol{p_e} = [p_{ex}, p_{ey}, p_{ez}]^T = \boldsymbol{p} - \boldsymbol{p_c}$ and $\boldsymbol{v_e} = [v_{ex}, v_{ey}, v_{ez}]^T = \boldsymbol{v} - \dot{\boldsymbol{p}}_{\boldsymbol{c}}$. From (3) and (10), the position error dynamics are derived as

$$\dot{\boldsymbol{p}}_{\boldsymbol{e}} = \boldsymbol{v_e}, \tag{13a}$$

$$\dot{\boldsymbol{v}}_{\boldsymbol{e}} = -g\boldsymbol{e_3} + \boldsymbol{U} - \ddot{\boldsymbol{p}}_{\boldsymbol{c}} + \boldsymbol{\Delta}_{\boldsymbol{f}}, \tag{13b}$$

Further, define the estimation and estimation error of $\boldsymbol{\sigma}$ as $\hat{\boldsymbol{\sigma}}$ and $\tilde{\boldsymbol{\sigma}} = \hat{\boldsymbol{\sigma}} - \boldsymbol{\sigma}$. Hyperbolic tangent functions are introduced here to establish the position loop control:

$$\begin{aligned}\boldsymbol{U} = {} & g\,\boldsymbol{e_3} + \ddot{\boldsymbol{p}}_{\boldsymbol{c}} - \alpha_p \mathbf{tanh}(k_p \boldsymbol{p_e} + l_p \boldsymbol{v_e}) \\ & - \beta_p \mathbf{tanh}(l_p \boldsymbol{v_e}) - \mathbf{Tanh}\left(\frac{\boldsymbol{\vartheta_f}}{\epsilon_f}\right)\hat{\boldsymbol{\sigma}},\end{aligned} \tag{14}$$

where α_p, β_p, k_p, l_p, $\epsilon_f > 0$, $\boldsymbol{\vartheta_f} = \alpha_p l_p \mathbf{tanh}(k_p \boldsymbol{p_e} + l_p \boldsymbol{v_e}) + \beta_p l_p \mathbf{tanh}(l_p \boldsymbol{v_e}) + k_p \boldsymbol{v_e}$ and $\hat{\boldsymbol{\sigma}} = [\hat{\sigma}_x, \hat{\sigma}_y, \hat{\sigma}_z]^T$ is obtained with the adaptive law:

$$\dot{\hat{\sigma}}_i = \begin{cases} \gamma_f \tan h\left(\frac{\vartheta_{fi}}{\epsilon_f}\right)\vartheta_{fi}, & |\hat{\sigma}_i| < \kappa_{fi}, \\ 0, & |\hat{\sigma}_i| = \kappa_{fi} \end{cases}, \quad i = x, y, z, \tag{15}$$

with $\gamma_f > 0$, and $\boldsymbol{\kappa_f} = [\kappa_{fx}, \kappa_{fy}, \kappa_{fz}]^T$ as an estimation upper bound.

Based on an integral-quadratic Lyapunov function, the stability of the position loop is acquired:

Theorem 1 *Consider the position error dynamics (13) with $\boldsymbol{\Delta}_f$ satisfying Assumption 1. The control (14) with the adaptive law (15) can guarantee that*

(i) $\boldsymbol{p_e}$ and $\boldsymbol{v_e}$ are bounded and ultimately converge to a neighborhood of the origin;
(ii) $|\hat{\sigma}_i| \le \kappa_{fi}$ $(i = x, y, z)$ holds if $|\hat{\sigma}_i(0)| \le \kappa_{fi}$.

Proof (i) Denote $\boldsymbol{\mu_1} = k_p \boldsymbol{p_e} + l_p \boldsymbol{v_e}$, $\boldsymbol{\mu_2} = l_p \boldsymbol{v_e}$ and $\boldsymbol{\mu} = [\boldsymbol{\mu_1}^T, \boldsymbol{\mu_2}^T]^T$. Designate a convergent set $\mathcal{Z}_{\mu 1} = \{\boldsymbol{\mu} \in \mathbb{R}^6 | \|\boldsymbol{\mu}\| < \bar{\mu}, \bar{\mu} > 0\}$. From Property 1, there exists a constant $\chi(\bar{\mu}) \in (0, 1)$ such that $\chi\|\boldsymbol{\mu}\| \le \|\mathbf{tanh}(\boldsymbol{\mu})\|$.

Substituting the control (14) into (13) yields

$$\dot{\boldsymbol{p}}_{\boldsymbol{e}} = \boldsymbol{v_e}, \tag{16a}$$

$$\begin{aligned}\dot{\boldsymbol{v}}_{\boldsymbol{e}} = {} & -\alpha_p \mathbf{tanh}(\boldsymbol{\mu_1}) - \beta_p \mathbf{tanh}(\boldsymbol{\mu_2}) \\ & - \mathbf{Tanh}\left(\frac{\boldsymbol{\vartheta_f}}{\epsilon_f}\right)\hat{\boldsymbol{\sigma}} + \boldsymbol{\Delta}_{\boldsymbol{f}}.\end{aligned} \tag{16b}$$

Assign the following integral-quadratic Lyapunov function candidate

$$L_p = \alpha_p \int_{\mathbf{0}}^{\boldsymbol{\mu_1}} \mathbf{tanh}(\boldsymbol{\xi}) d\boldsymbol{\xi} + \beta_p \int_{\mathbf{0}}^{\boldsymbol{\mu_2}} \mathbf{tanh}(\boldsymbol{\xi}) d\boldsymbol{\xi} + \frac{k_p}{2} \boldsymbol{v_e}^T \boldsymbol{v_e} + \frac{1}{2\gamma_f} \tilde{\boldsymbol{\sigma}}_f^T \tilde{\boldsymbol{\sigma}}_f > 0, \tag{17}$$

and its derivative along (16) satisfies

$$\begin{aligned}\dot{L}_p &= \alpha_p k_p \mathbf{tanh}^T(\boldsymbol{\mu_1}) \dot{\boldsymbol{p}}_e + \boldsymbol{\vartheta}_f^T \dot{\boldsymbol{v}}_e + \frac{1}{\gamma_f} \tilde{\boldsymbol{\sigma}}_f^T \dot{\hat{\boldsymbol{\sigma}}}_f \\ &= \alpha_p k_p \mathbf{tanh}^T(\boldsymbol{\mu_1}) \boldsymbol{v_e} + \boldsymbol{\vartheta}_f^T \left[-\alpha_p \mathbf{tanh}(\boldsymbol{\mu_1}) \right. \\ &\quad \left. -\beta_p \mathbf{tanh}(\boldsymbol{\mu_2}) - \mathbf{Tanh}\left(\frac{\boldsymbol{\vartheta}_f}{\epsilon_f}\right) \hat{\boldsymbol{\sigma}} + \boldsymbol{\Delta}_f \right] \\ &\quad + \frac{1}{\gamma_f} \tilde{\boldsymbol{\sigma}}_f^T \dot{\hat{\boldsymbol{\sigma}}}_f.\end{aligned}$$

According to Assumption 1 and Lemma 1,

$$\begin{aligned}\boldsymbol{\vartheta}_f^T \boldsymbol{\Delta}_f &\le \sum_{i=x,y,z} |\vartheta_{fi}| \sigma_i \\ &\le \sum_{i=x,y,z} \left[\vartheta_{fi} \tanh\left(\frac{\vartheta_{fi}}{\epsilon_f}\right) + k_q \epsilon_f \right] \sigma_i \\ &= \boldsymbol{\vartheta}_f^T \mathbf{Tanh}\left(\frac{\boldsymbol{\vartheta}_f}{\epsilon_f}\right) \boldsymbol{\sigma} + k_q \epsilon_f \sum_{i=x,y,z} \sigma_i.\end{aligned}$$

Then, $\dot{L}_p$ satisfies

$$\begin{aligned}\dot{L}_p \le & -l_p [\alpha_p \mathbf{tanh}(\boldsymbol{\mu}_1) + \beta_p \mathbf{tanh}(\boldsymbol{\mu}_2)]^T [\alpha_p \mathbf{tanh}(\boldsymbol{\mu}_1) \\ & + \beta_p \mathbf{tanh}(\boldsymbol{\mu}_2)] - k_p \beta_p \boldsymbol{v}_e^T \mathbf{tanh}(\boldsymbol{\mu}_2) \\ & + \tilde{\boldsymbol{\sigma}}^T \left[\frac{1}{\gamma_f} \dot{\hat{\boldsymbol{\sigma}}} - \mathbf{Tanh}\left(\frac{\boldsymbol{\vartheta}_f}{\epsilon_f}\right) \boldsymbol{\vartheta}_f \right] + d_f\end{aligned}$$

where $d_f = k_q \epsilon_f \sum_{i=x,y,z} \sigma_i$. According to [21], (15) can guarantee $\tilde{\boldsymbol{\sigma}}^T [\frac{1}{\gamma_f} \dot{\hat{\boldsymbol{\sigma}}} - \mathbf{Tanh}(\frac{\boldsymbol{\vartheta}_f}{\epsilon_f}) \boldsymbol{\vartheta}_f] \le 0$. Substituting (15) into the above inequality yields

$$\begin{aligned}\dot{L}_p \le & -l_p [\alpha_p \mathbf{tanh}(\boldsymbol{\mu}_1) + \beta_p \mathbf{tanh}(\boldsymbol{\mu}_2)]^T [\alpha_p \mathbf{tanh}(\boldsymbol{\mu}_1) \\ & + \beta_p \mathbf{tanh}(\boldsymbol{\mu}_2)] - k_p \beta_p \boldsymbol{v}_e^T \mathbf{tanh}(\boldsymbol{\mu}_2) + d_f \\ = & -\mathbf{tanh}(\boldsymbol{\mu})^T \boldsymbol{\Theta} \mathbf{tanh}(\boldsymbol{\mu}) + d_f,\end{aligned}$$

where

$$\boldsymbol{\Theta} = \begin{bmatrix} \alpha_p^2 l_p \boldsymbol{I_3} & \alpha_p \beta_p l_p \boldsymbol{I_3} \\ \alpha_p \beta_p l_p \boldsymbol{I_3} & \left(\beta_p^2 l_p + \frac{k_p \beta_p}{l_p}\right) \boldsymbol{I_3} \end{bmatrix}.$$

Since there exists an invertible matrix

$$\boldsymbol{T} = \begin{bmatrix} \boldsymbol{I_3} & -\frac{\beta_p}{\alpha_p} \boldsymbol{I_3} \\ \mathbf{0} & \boldsymbol{I_3} \end{bmatrix},$$

such that

$$\boldsymbol{T}^T \boldsymbol{\Theta} \boldsymbol{T} = \begin{bmatrix} \alpha_p^2 l_p \boldsymbol{I_3} & \mathbf{0} \\ \mathbf{0} & \frac{k_p \beta_p}{l_p} \boldsymbol{I_3} \end{bmatrix},$$

$\dot{L}_p$ satisfies

$$\dot{L}_p \le -\chi_2 \|\boldsymbol{\mu}\|^2 + d_f \tag{18}$$

where $\chi_2 = \min(\alpha_p^2 l_p \chi^2, \frac{k_p \beta_p}{l_p} \chi^2) > 0$. Thus, $\boldsymbol{\mu}$ is bounded and ultimately converges to the set:

$$\mathcal{Z}_{\mu 2} = \left\{ \boldsymbol{\mu} \in \mathbb{R}^6 \,|\, \|\boldsymbol{\mu}\| < \sqrt{\frac{d_f}{\chi_2}} \right\}. \tag{19}$$

Moreover, in order for $\boldsymbol{\mu} \in \mathcal{Z}_{\mu 1}$, it is required that $\sup(d_f) \le \chi_2 \bar{\mu}^2$. With a sufficiently small ϵ_f, d_f can be made arbitrarily small, which implies that an appropriate ϵ_f can guarantee $\boldsymbol{\mu}$ ultimately converging to $\mathcal{Z}_{\mu 2} \subseteq \mathcal{Z}_{\mu 1}$. Finally, it follows the definition of $\boldsymbol{\mu}$ that $\boldsymbol{p_e}$ and $\boldsymbol{v_e}$ are bounded and ultimately converge to the sets $\mathcal{Z}_p = \{\boldsymbol{p_e} \in \mathbb{R}^3 | \|\boldsymbol{p_e}\| < \frac{1}{k_p} \sqrt{\frac{d_f}{\chi_2}}\}$ and $\mathcal{Z}_v = \{\boldsymbol{v_e} \in \mathbb{R}^3 | \|\boldsymbol{v_e}\| < \frac{1}{l_p} \sqrt{\frac{d_f}{\chi_2}}\}$, respectively.

(ii) In terms of $|\hat{\sigma}_i(0)| \le \kappa_{fi}$ $(i = x, y, z)$, assign a Lyapunov function candidate $L_\sigma = \frac{1}{2} \hat{\sigma}_i^2$.

(a) If $|\hat{\sigma}_i| < \kappa_{fi}$, the conclusion is obvious.
(b) If $|\hat{\sigma}_i| = \kappa_{fi}$, then $\dot{L}_\sigma = 0$, so that $\hat{\sigma}_i$ is invariant.

Thus, $|\hat{\sigma}_i| \le \kappa_{fi}$ $(i = x, y, z)$ is warranted.

Due to $\|\boldsymbol{Re_3}\| = 1$, we derive the main rotor thrust:

$$T_m = m \|\boldsymbol{U}\|. \tag{20}$$

3.2 Attitude extraction

In terms of the hierarchical control strategy, extracting the command attitude from $\frac{T_m}{m} \boldsymbol{Re_3}$ is inevitable, whatever it is represented by the Euler angle [8] or unit quaternion [11,12]. In this subsection, the minimum rotation principle is employed to extract the command rotation matrix. Define $\boldsymbol{V} = \frac{T_m}{m} \boldsymbol{e_3} = [0, 0, \frac{T_m}{m}]^T$, which satisfies $\boldsymbol{RV} = \boldsymbol{U}$ and $\|\boldsymbol{U}\| = \|\boldsymbol{V}\|$.

Lemma 3 *Consider the position loop control (14). If* $\boldsymbol{U} \notin \mathcal{L} = \{\boldsymbol{U} \in \mathbb{R}^3 \mid \boldsymbol{U} = [0, 0, U_z]^T, U_z \le 0\}$, *the command rotation matrix* $\boldsymbol{R_c}$ *can be extracted as*

$$\boldsymbol{R_c} = \frac{m}{T_m}\begin{bmatrix} U_z + \frac{mU_y^2}{T_m+mU_z} & -\frac{mU_xU_y}{T_m+mU_z} & U_x \\ -\frac{mU_xU_y}{T_m+mU_z} & U_z + \frac{mU_x^2}{T_m+mU_z} & U_y \\ -U_x & -U_y & U_z \end{bmatrix}. \quad (21)$$

Proof In view of the minimum rotation principle, the principle rotation axis $\hat{\boldsymbol{k}}_{\boldsymbol{c}}$ is orthogonal to the plane composed by $\boldsymbol{U}$ and $\boldsymbol{V}$. Thus, we have

$$\begin{cases} \boldsymbol{U}^T\boldsymbol{V} = \|\boldsymbol{U}\|\|\boldsymbol{V}\|\cos\phi_c, \\ \boldsymbol{U}^\times\boldsymbol{V} = \|\boldsymbol{U}\|\|\boldsymbol{V}\|\sin\phi_c\hat{\boldsymbol{k}}_{\boldsymbol{c}}, \end{cases} \quad (22)$$

where ϕ_c is the rotation angle. If $\boldsymbol{U} \notin \mathcal{L}$, it follows $\|\boldsymbol{U}\| = \|\boldsymbol{V}\|$ that

$$\begin{cases} \cos\phi_c = \frac{\boldsymbol{U}^T\boldsymbol{V}}{\|\boldsymbol{U}\|\|\boldsymbol{V}\|} = \frac{mU_z}{T_m}, \\ \sin\phi_c = \sqrt{1-\cos^2\phi_c} = \frac{\sqrt{T_m^2-m^2U_z^2}}{T_m}, \\ \hat{\boldsymbol{k}}_{\boldsymbol{c}} = \frac{\boldsymbol{U}^\times\boldsymbol{V}}{\|\boldsymbol{U}\|\|\boldsymbol{V}\|\sin\phi_c} = \frac{m}{\sqrt{T_m^2-m^2U_z^2}}\begin{bmatrix} U_y \\ -U_x \\ 0 \end{bmatrix}. \end{cases} \quad (23)$$

Based on the Euler's formula [28], we have

$$\boldsymbol{R_c} = \cos\phi_c\boldsymbol{I_3} + (1-\cos\phi_c)\hat{\boldsymbol{k}}_{\boldsymbol{c}}\hat{\boldsymbol{k}}_{\boldsymbol{c}}^T - \sin\phi_c\hat{\boldsymbol{k}}_{\boldsymbol{c}}^\times. \quad (24)$$

Substituting (23) into (24) and conducting some analytical computations, we can derive (21).

Remark 2 In order for $\boldsymbol{U} \notin \mathcal{L}$, the reference acceleration $\ddot{\boldsymbol{p}}_{\boldsymbol{c}} = [\ddot{p}_{cx}, \ddot{p}_{cy}, \ddot{p}_{cz}]^T$, the control parameters α_p and β_p, and the upper bound $\boldsymbol{\kappa_f}$ are supposed to satisfy one of the following conditions:

(a) $\alpha_p + \beta_p + \kappa_{fx} < |\ddot{p}_{cx}(t)|, \quad \forall t \geq 0;$
(b) $\alpha_p + \beta_p + \kappa_{fy} < |\ddot{p}_{cy}(t)|, \quad \forall t \geq 0;$
(c) $\alpha_p + \beta_p + \kappa_{fz} < g - \delta$ and $|\ddot{p}_{cz}(t)| < \delta, \quad \forall t \geq 0.$

During the low-speed flight, $\ddot{\boldsymbol{p}}_{\boldsymbol{c}}$ is small, and Conditions (a) and (b) constrain the parameter choice greatly. Condition (c) is the criterion for choosing the parameters.

3.3 Attitude loop control design

To proceed, the command angular velocity $\boldsymbol{\omega_c}$ and its derivative $\dot{\boldsymbol{\omega}}_{\boldsymbol{c}}$ are required, which are derived in Appendix A. Determining $\boldsymbol{\omega_c}$ and $\dot{\boldsymbol{\omega}}_{\boldsymbol{c}}$ needs the knowledge of $\dot{\boldsymbol{U}}$ and $\ddot{\boldsymbol{U}}$, which are intricate to be acquired with analytical calculations. Alternatively, a command filter [29] is applied to approximate them.

Define the attitude and angular velocity tracking errors as $\boldsymbol{R_e} = \boldsymbol{R_c}^T\boldsymbol{R} \in SO(3)$ and $\boldsymbol{\omega_e} = \boldsymbol{\omega} - \boldsymbol{R_e}^T\boldsymbol{\omega_c}$. $\boldsymbol{R_e} = \boldsymbol{I_3}$ means $\boldsymbol{R} = \boldsymbol{R_c}$, namely the exact attitude tracking. Due to dimensional inconsistency, it is hard to design an attitude loop control with $\boldsymbol{R_e}$ directly. Instead, a new attitude error representation [19] is introduced:

$$\boldsymbol{e_R} = \frac{1}{2\sqrt{1+\mathrm{tr}(\boldsymbol{R_e})}}(\boldsymbol{R_e} - \boldsymbol{R_e}^T)^\vee. \quad (25)$$

With $\mathrm{tr}(\boldsymbol{R_e}) \neq -1$, $\boldsymbol{e_R} = \boldsymbol{0}$ is equivalent to $\boldsymbol{R_e} = \boldsymbol{I_3}$. Then, the attitude error dynamics satisfy

$$\dot{\boldsymbol{e}}_{\boldsymbol{R}} = \boldsymbol{\Omega}\boldsymbol{\omega_e}, \quad (26a)$$

$$\boldsymbol{J}\dot{\boldsymbol{\omega}}_{\boldsymbol{e}} = -\boldsymbol{\omega}^\times\boldsymbol{J}\boldsymbol{\omega} + \boldsymbol{\tau_c} + \boldsymbol{\Delta_\tau} + \boldsymbol{J}\boldsymbol{\omega_e}^\times\boldsymbol{R_e}^T\boldsymbol{\omega_c} - \boldsymbol{J}\boldsymbol{R_e}^T\dot{\boldsymbol{\omega}}_{\boldsymbol{c}}, \quad (26b)$$

where $\boldsymbol{\Omega} = \frac{1}{2\sqrt{1+\mathrm{tr}(\boldsymbol{R_e})}}(\mathrm{tr}(\boldsymbol{R_e})\boldsymbol{I_3} - \boldsymbol{R_e}^T + 2\boldsymbol{e_R}\boldsymbol{e_R}^T)$ is nonsingular when $\mathrm{tr}(\boldsymbol{R_e}) \neq -1$ or $\boldsymbol{R_c} \neq -\boldsymbol{R}$. According to [30], $\mathbf{tr}(\boldsymbol{R_e}) \neq -1$ is equivalent to $\|\boldsymbol{e_R}\| < 1$.

Let $\tilde{\boldsymbol{\omega}} = [\tilde{\omega}_x, \tilde{\omega}_y, \tilde{\omega}_z]^T = \boldsymbol{\omega_e} - \boldsymbol{\alpha_R}$, where $\boldsymbol{\alpha_R}$ is a virtual control, determined by

$$\boldsymbol{\alpha_R} = -k_R\boldsymbol{\Omega}^{-1}\boldsymbol{e_R}, k_R > 0. \quad (27)$$

Further, define the estimation and estimation error of $\boldsymbol{\varsigma}$ as $\hat{\boldsymbol{\varsigma}}$ and $\tilde{\boldsymbol{\varsigma}} = \hat{\boldsymbol{\varsigma}} - \boldsymbol{\varsigma}$. Design the attitude loop control:

$$\boldsymbol{\tau_c} = -k_\omega\tilde{\boldsymbol{\omega}} + \boldsymbol{\omega}^\times\boldsymbol{J}\boldsymbol{\omega} - \boldsymbol{J}\boldsymbol{\omega_e}^\times\boldsymbol{R_e}^T\boldsymbol{\omega_c} + \boldsymbol{J}\boldsymbol{R_e}^T\dot{\boldsymbol{\omega}}_{\boldsymbol{c}} + \boldsymbol{J}\dot{\boldsymbol{\alpha}}_{\boldsymbol{R}} - \frac{\boldsymbol{\Omega}^T\boldsymbol{e_R}}{1-\|\boldsymbol{e_R}\|^2} - \mathbf{Tanh}\left(\frac{\tilde{\boldsymbol{\omega}}}{\epsilon_\tau}\right)\hat{\boldsymbol{\varsigma}} \quad (28)$$

where $k_\omega, \epsilon_\tau > 0$, and $\hat{\boldsymbol{\varsigma}} = [\hat{\varsigma}_x, \hat{\varsigma}_y, \hat{\varsigma}_z]^T$ is obtained with the adaptive law:

$$\dot{\hat{\varsigma}}_i = \gamma_{\tau 1}\left[\tanh\left(\frac{\tilde{\omega}_i}{\epsilon_\tau}\right)\tilde{\omega}_i - \gamma_{\tau 2}\hat{\varsigma}_i\right], \quad i = x, y, z, \quad (29)$$

with $\gamma_{\tau 1}, \gamma_{\tau 2} > 0$.

Based on a barrier-quadratic Lyapunov function, the stability of the attitude loop is acquired:

Theorem 2 *Consider the attitude error dynamics (26) with $\boldsymbol{\Delta_\tau}$ satisfying Assumption 1. If the initial rotation matrix satisfies $\boldsymbol{R}(0) \neq -\boldsymbol{R_c}(0)$, then the control (28) with the adaptive law (29) can guarantee that*

(i) $\boldsymbol{e_R}$ always remains in $\mathcal{Z}_{R1} = \{\boldsymbol{e_R} \in \mathbb{R}^3 | \|\boldsymbol{e_R}\| < 1\}$;

(ii) $\boldsymbol{e_R}$ *and* $\tilde{\boldsymbol{\omega}}$ *are bounded and ultimately converge to a neighborhood of the origin.*

Proof Assign the following barrier-quadratic Lyapunov function candidate

$$L_a = \frac{1}{2}\ln\frac{1}{1-\|\boldsymbol{e_R}\|^2} + \frac{1}{2}\tilde{\boldsymbol{\omega}}^T\boldsymbol{J}\tilde{\boldsymbol{\omega}} + \frac{1}{2\gamma_{\tau 1}}\tilde{\boldsymbol{\varsigma}}^T\tilde{\boldsymbol{\varsigma}}, \quad (30)$$

which, according to Lemma 2, satisfies

$$L_a \le \frac{1}{2}\frac{\|\boldsymbol{e_R}\|^2}{1-\|\boldsymbol{e_R}\|^2} + \frac{1}{2}\tilde{\boldsymbol{\omega}}^T\boldsymbol{J}\tilde{\boldsymbol{\omega}} + \frac{1}{2\gamma_{\tau 1}}\tilde{\boldsymbol{\varsigma}}^T\tilde{\boldsymbol{\varsigma}}. \quad (31)$$

Differentiating L_a along (26) yields

$$\begin{aligned}\dot{L}_a &= \frac{\boldsymbol{e_R}^T\boldsymbol{\Omega}}{1-\|\boldsymbol{e_R}\|^2}\dot{\boldsymbol{e}}_{\boldsymbol{R}} + \tilde{\boldsymbol{\omega}}^T\boldsymbol{J}\dot{\tilde{\boldsymbol{\omega}}} + \frac{1}{\gamma_{\tau 1}}\tilde{\boldsymbol{\varsigma}}^T\dot{\tilde{\boldsymbol{\varsigma}}}\\ &= \frac{\boldsymbol{e_R}^T\boldsymbol{\Omega}}{1-\|\boldsymbol{e_R}\|^2}(\boldsymbol{\alpha_R}+\tilde{\boldsymbol{\omega}}) + \tilde{\boldsymbol{\omega}}^T(-\boldsymbol{\omega}^{\times}\boldsymbol{J}\boldsymbol{\omega}\\ &\quad +\boldsymbol{J}\boldsymbol{\omega_e}^{\times}\boldsymbol{R}_{\boldsymbol{e}}^T\boldsymbol{\omega_c} - \boldsymbol{J}\boldsymbol{R}_{\boldsymbol{e}}^T\dot{\boldsymbol{\omega}}_{\boldsymbol{c}}\\ &\quad +\boldsymbol{\tau_c}+\boldsymbol{\Delta_\tau}-\boldsymbol{J}\dot{\boldsymbol{\alpha}}_{\boldsymbol{R}}) + \frac{1}{\gamma_{\tau 1}}\tilde{\boldsymbol{\varsigma}}^T\dot{\tilde{\boldsymbol{\varsigma}}}. \end{aligned} \quad (32)$$

Substituting (27) into (32) yields

$$\begin{aligned}\dot{L}_a &= -k_R\frac{\boldsymbol{e_R}^T\boldsymbol{e_R}}{1-\|\boldsymbol{e_R}\|^2} + \tilde{\boldsymbol{\omega}}^T\left(-\boldsymbol{\omega}^{\times}\boldsymbol{J}\boldsymbol{\omega}\right.\\ &\quad +\boldsymbol{\tau_c}+\boldsymbol{J}\boldsymbol{\omega_e}^{\times}\boldsymbol{R}_{\boldsymbol{e}}^T\boldsymbol{\omega_c} - \boldsymbol{J}\boldsymbol{R}_{\boldsymbol{e}}^T\dot{\boldsymbol{\omega}}_{\boldsymbol{c}}\\ &\quad \left.-\boldsymbol{J}\dot{\boldsymbol{\alpha}}_{\boldsymbol{R}}+\boldsymbol{\Delta_\tau}+\frac{\boldsymbol{\Omega}^T\boldsymbol{e_R}}{1-\|\boldsymbol{e_R}\|^2}\right) + \frac{1}{\gamma_{\tau 1}}\tilde{\boldsymbol{\varsigma}}^T\dot{\tilde{\boldsymbol{\varsigma}}}. \end{aligned}$$

According to Assumption 1 and Lemma 1,

$$\begin{aligned}\tilde{\boldsymbol{\omega}}^T\boldsymbol{\Delta_\tau} &\le \sum_{i=x,y,z}|\tilde{\omega}_i|\varsigma_i\\ &\le \sum_{i=x,y,z}\left[\tilde{\omega}_i\tanh\left(\frac{\tilde{\omega}_i}{\epsilon_\tau}\right)+k_q\epsilon_\tau\right]\varsigma_i\\ &= \tilde{\boldsymbol{\omega}}^T\mathbf{Tanh}\left(\frac{\tilde{\boldsymbol{\omega}}}{\epsilon_\tau}\right)\boldsymbol{\varsigma} + k_q\epsilon_\tau\sum_{i=x,y,z}\varsigma_i. \end{aligned}$$

Then, $\dot{L}_a$ satisfies

$$\begin{aligned}\dot{L}_a &\le -k_R\frac{\boldsymbol{e_R}^T\boldsymbol{e_R}}{1-\|\boldsymbol{e_R}\|^2} + \tilde{\boldsymbol{\varsigma}}^T\left[\frac{1}{\gamma_{\tau 1}}\dot{\tilde{\boldsymbol{\varsigma}}} - \mathbf{Tanh}\left(\frac{\tilde{\boldsymbol{\omega}}}{\epsilon_\tau}\right)\tilde{\boldsymbol{\omega}}\right]\\ &\quad +\tilde{\boldsymbol{\omega}}^T\left[-\boldsymbol{\omega}^{\times}\boldsymbol{J}\boldsymbol{\omega}+\boldsymbol{\tau_c}+\boldsymbol{J}\boldsymbol{\omega_e}^{\times}\boldsymbol{R}_{\boldsymbol{e}}^T\boldsymbol{\omega_c} - \boldsymbol{J}\boldsymbol{R}_{\boldsymbol{e}}^T\dot{\boldsymbol{\omega}}_{\boldsymbol{c}}\right.\\ &\quad \left.-\boldsymbol{J}\dot{\boldsymbol{\alpha}}_{\boldsymbol{R}}+\frac{\boldsymbol{\Omega}^T\boldsymbol{e_R}}{1-\|\boldsymbol{e_R}\|^2}+\mathbf{Tanh}\left(\frac{\tilde{\boldsymbol{\omega}}}{\epsilon_\tau}\right)\hat{\boldsymbol{\varsigma}}\right] + \bar{d}_\tau, \end{aligned} \quad (33)$$

where $\bar{d}_\tau = k_q\epsilon_\tau\sum_{i=x,y,z}\varsigma_i$. Substituting (28) and (29) into (33) yields

$$\begin{aligned}\dot{L}_a &\le -k_R\frac{\boldsymbol{e_R}^T\boldsymbol{e_R}}{1-\|\boldsymbol{e_R}\|^2} - k_\omega\tilde{\boldsymbol{\omega}}^T\tilde{\boldsymbol{\omega}} - \gamma_{\tau 2}\tilde{\boldsymbol{\varsigma}}^T\hat{\boldsymbol{\varsigma}} + \bar{d}_\tau\\ &\le -k_R\frac{\boldsymbol{e_R}^T\boldsymbol{e_R}}{1-\|\boldsymbol{e_R}\|^2} - k_\omega\tilde{\boldsymbol{\omega}}^T\tilde{\boldsymbol{\omega}} - \frac{\gamma_{\tau 2}}{2}\hat{\boldsymbol{\varsigma}}^T\hat{\boldsymbol{\varsigma}} + d_\tau\\ &\le -k_\tau L_a + d_\tau, \end{aligned} \quad (34)$$

where $k_\tau = \min(2k_R, 2\frac{k_\omega}{\bar{\lambda}(\boldsymbol{J})}, \frac{\gamma_{\tau 1}}{\gamma_{\tau 2}})$ and $d_\tau = \bar{d}_\tau + \frac{\gamma_{\tau 2}}{2}\boldsymbol{\varsigma}^T\boldsymbol{\varsigma}$.

(i) $\boldsymbol{R}(0) \ne -\boldsymbol{R_c}(0)$ means $\|\boldsymbol{e_R(0)}\| < 1$. Integrating both sides of (34) over $[0, t]$ gives

$$0 \le L_a(t) \le \left(L_a(0) - \frac{d_\tau}{k_\tau}\right)e^{-k_\tau t} + \frac{d_\tau}{k_\tau} \le L_a(0) + \frac{d_\tau}{k_\tau}, \quad (35)$$

which implies that L_a is bounded. From (30) and (35),

$$\frac{1}{2}\ln\frac{1}{1-\|\boldsymbol{e_R}\|^2} \le \left(L_a(0) - \frac{d_\tau}{k_\tau}\right)e^{-k_\tau t} + \frac{d_\tau}{k_\tau}. \quad (36)$$

Take exponentials on both sides of (36) and conduct some computations, then

$$\|\boldsymbol{e_R}(t)\| \le \sqrt{1 - e^{-2\left[\frac{d_\tau}{k_\tau} + \left(L_a(0) - \frac{d_\tau}{k_\tau}\right)\exp(-\frac{d_\tau}{k_\tau}t)\right]}} < 1, \quad (37)$$

which means that as long as $\|\boldsymbol{e_R(0)}\| < 1$ or $\boldsymbol{R}(0) \ne -\boldsymbol{R_c}(0)$, $\boldsymbol{e_R}(t)$ always remains in $\mathcal{Z}_{R1}$.

(ii) It follows (37) that $\boldsymbol{e_R}$ is bounded and ultimately converges to $\mathcal{Z}_{R2} = \left\{\boldsymbol{e_R} \in \mathbb{R}^3 | \|\boldsymbol{e_R}\| \le \sqrt{1 - e^{-2\frac{d_\tau}{k_\tau}}}\right\}$. In addition, from (30) and (35), $\tilde{\boldsymbol{\omega}}$ is bounded and ultimately converges to $\mathcal{Z}_\omega = \{\tilde{\boldsymbol{\omega}} \in \mathbb{R}^3 | \|\tilde{\boldsymbol{\omega}}\| \le \sqrt{\frac{2d_\tau}{\underline{\lambda}(\boldsymbol{J})k_\tau}}\}$.

Remark 3 Given $\ddot{\boldsymbol{p}}_{\boldsymbol{c}}$, $\dot{\boldsymbol{p}}_{\boldsymbol{c}}$, $\boldsymbol{p_c}$, $\boldsymbol{p}(0)$, $\boldsymbol{v}(0)$ and $\hat{\boldsymbol{\sigma}}(0)$, initial $\boldsymbol{U}(0)$ can be determined by (14). Then initial $\boldsymbol{R_c}(0)$ can be determined by (21). Thus, the initial rotation matrix $\boldsymbol{R}(0) \ne -\boldsymbol{R_c}(0)$ can be chosen easily.

In addition, from (9), we derive $\boldsymbol{M} = [T_t, a_s, b_s]^T$ as

$$\boldsymbol{M} = \boldsymbol{\tau_A}^{-1}(\boldsymbol{\tau_c} - \boldsymbol{\tau_B}). \quad (38)$$

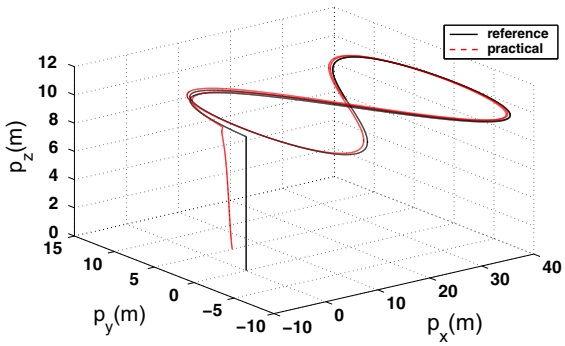

Fig. 2 3D trajectory tracking

4 Simulations

In order to verify the effectiveness of the proposed adaptive control approach, some simulations are conducted for a model-scaled helicopter with MATLAB/Simulink. The parameters of the helicopter are introduced from [31]. The reference trajectory consists of two parts: First, the helicopter lifts vertically for the first 10 s; then, it conducts an "8-shaped" curve fight to the end. Specifically, the reference trajectory is described as

$$\boldsymbol{p_c}(t) = \begin{cases} [0, 0, 10(1 - e^{-0.3t})]^T m & \text{if } t \leq 10 \text{ s} \\ \begin{bmatrix} 20(1 - \cos\frac{2\pi}{23}(t-10)), \\ 10\sin\left(\frac{4\pi}{23}(t-10)\right), \\ 10(1 - e^{-0.3t}) \end{bmatrix} m & \text{otherwise} \end{cases}$$

The helicopter is initially still at $\boldsymbol{p}(0) = [5, 5, 0]^T$ with the initial rotation matrix $\boldsymbol{R}(0) = \boldsymbol{I_3}$. Besides, a 40% mass drop appears at 30 sec.

The attitude loop control parameters are required to be tuned sufficiently large, so that the helicopter can reach its command attitude rapidly. In terms of the position loop control parameters, they are tuned based on Condition (c) in Remark 2. In view of (15) and (29), they are both increasing functions with respect to ϑ_{fi}^2 and $\tilde{\omega}_i^2$ $(i = x, y, z)$, so that γ_f and $\gamma_{\tau 1}$ are required not too high. Specifically, the control and adaptive parameters are as follows: $l_p = 0.5$, $k_p = \alpha_p = 1$, $\beta_p = 4$, $k_R = k_\omega = 8$, $\gamma_f = \gamma_{\tau 1} = 0.02$, $\gamma_{\tau 2} = 2.5$ and $\epsilon_f = \epsilon_\tau = 0.02$. Further, we choose $\kappa_{fi} = 2$ $(i = x, y, z)$ to constrain the increment of $\hat{\sigma}_i$.

3D tracking figure in Fig. 2 illustrates that the trajectory tracking objective is accomplished with the proposed control approach. Figure 3 illustrates the

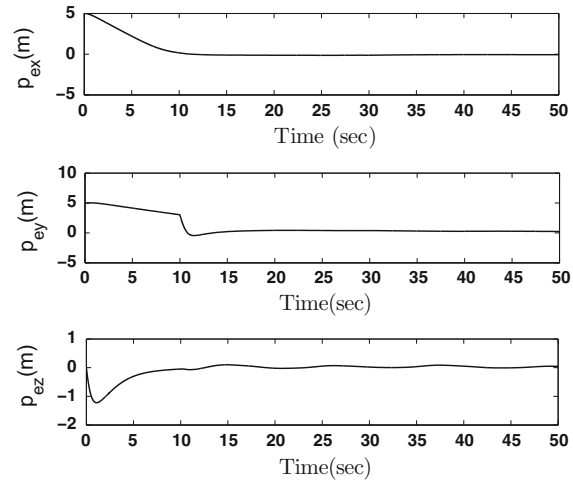

Fig. 3 Position tracking error

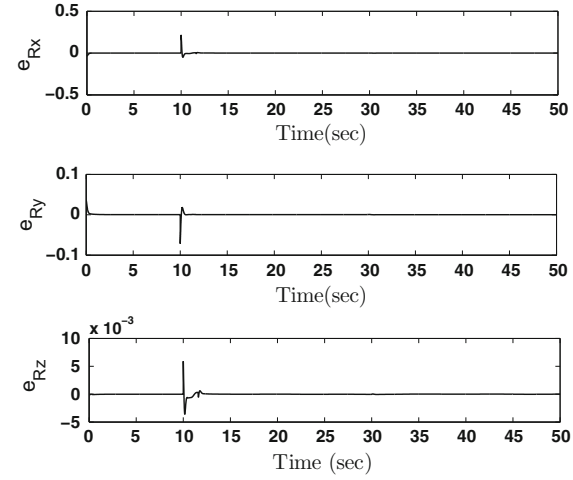

Fig. 4 Attitude tracking error

bounded position tracking error in spite of the mass drop, which demonstrates the robustness of the proposed control approach to the parameter uncertainty. Figure 4 illustrates the bounded attitude tracking error in spite of a large tracking error that appears at 10 sec due to a sudden turning. Then, Fig. 5 shows that $\|\boldsymbol{e_R}\|$ remains in the set $\mathcal{Z}_{R1}$ all the time, which implies that no singularity occurs during the tracking progress. From Figs. 6 and 7, $\boldsymbol{\sigma}$ satisfies $\sigma_i \leq \kappa_{fi}$ $(i = x, y, z)$ and $\boldsymbol{\varsigma}$ is bounded.

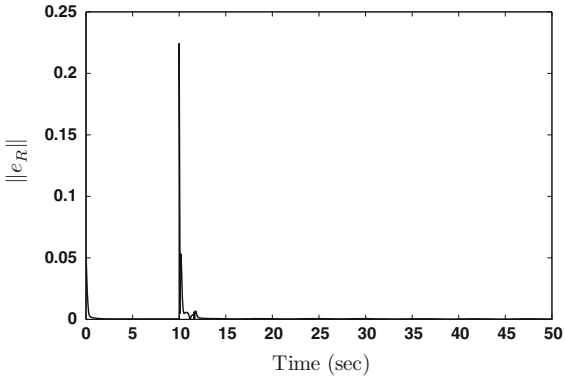

Fig. 5 $\|e_R\|$

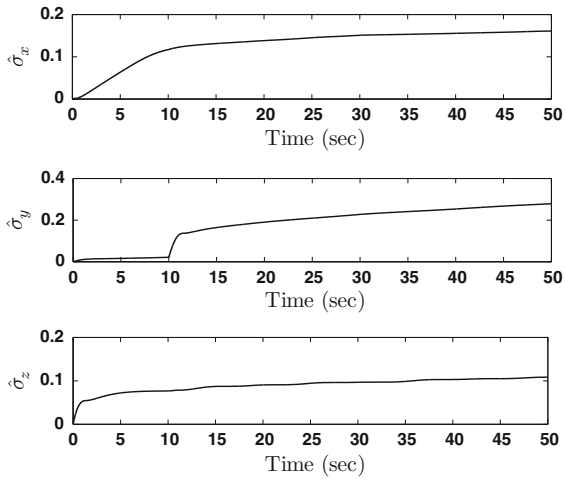

Fig. 6 $\hat{\sigma}$

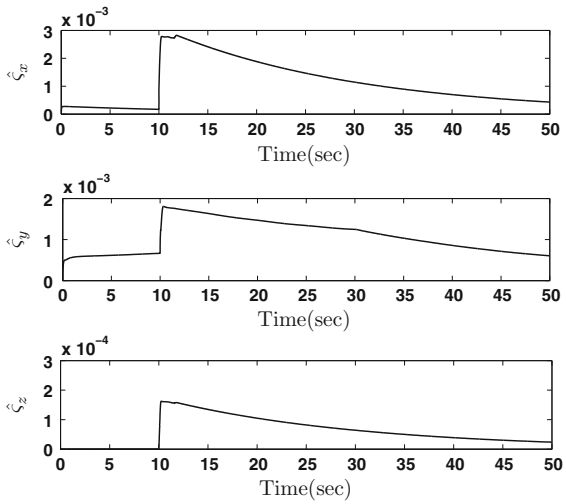

Fig. 7 $\hat{\varsigma}$

5 Conclusion

An adaptive trajectory tracking control approach is proposed for a model-scaled helicopter with the rotation matrix representing the attitude. Based on a decomposed model with the cascaded structure, the control approach is designed with the hierarchical architecture. The position and attitude loop control laws are designed based on integral-quadratic Lyapunov function and barrier-quadratic Lyapunov function, respectively. They respectively complete the position and attitude tracking missions without the singularity. The upper bounds of the unmodeled dynamics are estimated and compensated. Simulations verify the performance of the proposed control approach.

Acknowledgments The author sincerely appreciates his supervisor Prof. Wei Huo of the Seventh Research Division, Beihang University, for his suggestions and motivations.

Derivation of the desired angular velocity

The detailed derivation for the desired angular velocity $\boldsymbol{\omega_c} = [\omega_{cx}, \omega_{cy}, \omega_{cz}]^T$ and its derivative $\dot{\boldsymbol{\omega}}_{\boldsymbol{c}}$ are as follows.

From (20), we obtain

$$\boldsymbol{R_c e_3} = \frac{\boldsymbol{U}}{\sqrt{\boldsymbol{U}^T\boldsymbol{U}}}. \tag{39}$$

The first-order time derivatives of $\boldsymbol{R_c e_3}$ are derived as

$$\begin{aligned}\frac{\mathrm{d}}{\mathrm{d}t}(\boldsymbol{R_c e_3}) &= \frac{1}{\sqrt{\boldsymbol{U}^T\boldsymbol{U}}}\left(\boldsymbol{I_3} - \frac{\boldsymbol{U}\boldsymbol{U}^T}{\boldsymbol{U}^T\boldsymbol{U}}\right)\dot{\boldsymbol{U}} \\ &= \frac{1}{\|\boldsymbol{U}\|}\left(\boldsymbol{I_3} - \boldsymbol{R_c e_3 e_3^T R_c^T}\right)\dot{\boldsymbol{U}} \\ &= \frac{1}{\|\boldsymbol{U}\|}\boldsymbol{R_c \Pi R_c^T}\dot{\boldsymbol{U}},\end{aligned} \tag{40}$$

where $\boldsymbol{\Pi} = \boldsymbol{I_3} - \boldsymbol{e_3 e_3^T}$. Further, denote $\boldsymbol{R_c e_3} = [R_1, R_2, R_3]^T$. From (21), we have

$$\boldsymbol{R_c e_2} = \left[-\frac{R_1 R_2}{1+R_3}, R_3 + \frac{R_1^2}{1+R_3}, -R_2\right]^T. \tag{41}$$

The first-order time derivative of $\boldsymbol{R_c e_2}$ is derived as

$$\frac{\mathrm{d}}{\mathrm{d}t}(\boldsymbol{R_c e_2}) = \boldsymbol{\Theta}\frac{\mathrm{d}}{\mathrm{d}t}(\boldsymbol{R_c e_3}), \tag{42}$$

where

$$\boldsymbol{\Theta} = \begin{bmatrix} -\frac{R_2}{1+R_3} & -\frac{R_1}{1+R_3} & \frac{R_1 R_2}{(1+R_3)^2} \\ \frac{2R_1}{1+R_3} & 0 & 1-\frac{R_1^2}{(1+R_3)^2} \\ 0 & -1 & 0 \end{bmatrix}, \tag{43}$$

and its first-order time derivative is

$$\begin{aligned} \dot{\boldsymbol{\Theta}} = & \begin{bmatrix} 0 & -\frac{1}{1+R_3} & \frac{R_2}{(1+R_3)^2} \\ \frac{2}{1+R_3} & 0 & -\frac{2R_1}{(1+R_3)^2} \\ 0 & 0 & 0 \end{bmatrix} \frac{\mathrm{d}}{\mathrm{d}t}(\boldsymbol{R_c e_3}) \boldsymbol{e_1}^T \\ & + \begin{bmatrix} -\frac{1}{1+R_3} & 0 & \frac{R_1}{(1+R_3)^2} \\ 0 & 0 & 0 \\ 0 & 0 & 0 \end{bmatrix} \frac{\mathrm{d}}{\mathrm{d}t}(\boldsymbol{R_c e_3}) \boldsymbol{e_2}^T \\ & + \begin{bmatrix} \frac{R_2}{(1+R_3)^2} & \frac{R_1}{(1+R_3)^2} & -\frac{2R_1 R_2}{(1+R_3)^3} \\ -\frac{2R_1}{(1+R_3)^2} & 0 & \frac{2R_1^2}{(1+R_3)^3} \\ 0 & 0 & 0 \end{bmatrix} \\ & \times \frac{\mathrm{d}}{\mathrm{d}t}(\boldsymbol{R_c e_3}) \boldsymbol{e_3}^T. \end{aligned} \tag{44}$$

It follows (5) that $\frac{\mathrm{d}}{\mathrm{d}t}(\boldsymbol{R_c e_3}) = \boldsymbol{R_c} \boldsymbol{\omega_c}^{\times} \boldsymbol{e_3}$ and $\frac{\mathrm{d}}{\mathrm{d}t}(\boldsymbol{R_c e_2}) = \boldsymbol{R_c} \boldsymbol{\omega_c}^{\times} \boldsymbol{e_2}$, so that

$$\begin{aligned} \boldsymbol{\omega_c}^{\times} \boldsymbol{e_3} &= \begin{bmatrix} \omega_{cy} \\ -\omega_{cx} \\ 0 \end{bmatrix} = \boldsymbol{R_c}^T \frac{\mathrm{d}}{\mathrm{d}t}(\boldsymbol{R_c e_3}) \\ &= \frac{1}{\|\boldsymbol{U}\|} \boldsymbol{\Pi} \boldsymbol{R_c}^T \dot{\boldsymbol{U}}, \end{aligned} \tag{45}$$

$$\begin{aligned} \boldsymbol{\omega_c}^{\times} \boldsymbol{e_2} &= \begin{bmatrix} -\omega_{cz} \\ 0 \\ \omega_{cx} \end{bmatrix} = \boldsymbol{R_c}^T \frac{\mathrm{d}}{\mathrm{d}t}(\boldsymbol{R_c e_2}) \\ &= \frac{1}{\|\boldsymbol{U}\|} \boldsymbol{R_c}^T \boldsymbol{\Theta} \boldsymbol{\Lambda} \dot{\boldsymbol{U}}, \end{aligned} \tag{46}$$

where $\boldsymbol{\Lambda} = \boldsymbol{R_c} \boldsymbol{\Pi} \boldsymbol{R_c}^T$, and its first-order time derivative is

$$\begin{aligned} \dot{\boldsymbol{\Lambda}} &= \dot{\boldsymbol{R}}_{\boldsymbol{c}} \boldsymbol{\Pi} \boldsymbol{R_c}^T + \boldsymbol{R_c} \boldsymbol{\Pi} \dot{\boldsymbol{R}}_{\boldsymbol{c}}^T \\ &= \boldsymbol{R_c} \boldsymbol{\omega_c}^{\times} \boldsymbol{\Pi} \boldsymbol{R_c}^T - \boldsymbol{R_c} \boldsymbol{\Pi} \boldsymbol{\omega_c}^{\times} \boldsymbol{R_c}^T = \boldsymbol{0}. \end{aligned}$$

In addition, differentiating (45) and (46) yields

$$\dot{\boldsymbol{\omega}}_{\boldsymbol{c}}^{\times} \boldsymbol{e_3} = \frac{1}{\|\boldsymbol{U}\|} \boldsymbol{\Pi} \left[\dot{\boldsymbol{R}}_{\boldsymbol{c}}^T \dot{\boldsymbol{U}} + \boldsymbol{R_c}^T \left(\ddot{\boldsymbol{U}} - \frac{\boldsymbol{U}^T \dot{\boldsymbol{U}}}{\|\boldsymbol{U}\|^2} \dot{\boldsymbol{U}} \right) \right] \tag{47}$$

$$\begin{aligned} \dot{\boldsymbol{\omega}}_{\boldsymbol{c}}^{\times} \boldsymbol{e_2} = & \frac{1}{\|\boldsymbol{U}\|} \left[\left(\dot{\boldsymbol{R}}_{\boldsymbol{c}}^T \boldsymbol{\Theta} + \boldsymbol{R_c}^T \dot{\boldsymbol{\Theta}} \right) \boldsymbol{\Lambda} \dot{\boldsymbol{U}} \right. \\ & \left. + \boldsymbol{R_c}^T \boldsymbol{\Theta} \boldsymbol{\Lambda} \left(\ddot{\boldsymbol{U}} - \frac{\boldsymbol{U}^T \dot{\boldsymbol{U}}}{\|\boldsymbol{U}\|^2} \dot{\boldsymbol{U}} \right) \right] \end{aligned} \tag{48}$$

where $\dot{\boldsymbol{R}}_{\boldsymbol{c}}^T = -\boldsymbol{\omega_c} \times \boldsymbol{R_c}^T$.

References

1. Zhu, B., Huo, W.: Robust nonlinear control for a model-scaled helicopter with parameter uncertainties. Nonlinear Dyn. **73**, 1139–1154 (2013)
2. He, Y.B., Pei, H.L., Sun, T.R.: Robust tracking control of helicopter using backstepping with disturbance observers. Asian J. Control **16**(6), 1–16 (2014)
3. Johnson, E.N., Kannan, S.K.: Adaptive trajectory control for autonomous helicopters'. J. Guid. Control Dyn. **28**(3), 524–538 (2005)
4. Simplicio, P., Pavel, M.D., et al.: An acceleration measurements-based approach for helicopter nonlinear fight control using incremental nonlinear dynamic inversion. Control Eng. Pract. **21**(8), 1065–1077 (2013)
5. Samal, M.K., Garratt, M., et al.: Model predictive flight controller for longitudinal and lateral cyclic control of an unmanned helicopter. In: AUCC, Syndey, Australia, pp 386–391 (2012)
6. Raffo, G.V., Ortega, M.G., Rubio, F.R.: Path tracking of a UAV via an underactuated H_∞ control strategy. Eur. J. Control **17**(2), 194–213 (2011)
7. Hua, M.D., Hamel, T., et al.: Introduction to feedback control of underactuated VTOL vehicles: a review of basic control design ideas and principles. IEEE Trans. Control Syst. **33**(1), 61–75 (2013)
8. Zuo, Z.Y., Ru, P.K.: Augmented L_1 adaptive tracking control of quad-rotor unmanned aircrafts. IEEE Trans. Aerosp. Electron. Syst. **50**(4), 3090–3101 (2014)
9. Zuo, Z.Y., Ding, X.F.: Almost global trajectory tracking control of quadrotors with constrained control inputs. J. Aerosp. Eng. doi:10.1177/0954410015600461
10. Cabecinhas, D., Cunba, R., Silvestre, C.: A nonlinear quadrotor trajectory tracking controller with disturbance rejection. Control Eng. Pract. **26**, 1–10 (2014)
11. Abdessameud, A., Sharifi, F.J.: Image-based tracking control of VTOL unmanned aerial vehicles. Automatica **53**, 111–119 (2015)
12. Abdessameud, A., Tayebi, A.: Global trajectory tracking control of VTOL-UAVs without linear velocity measurements. Automatica **46**(6), 1053–1059 (2010)
13. Lee, T.L.: Robust adaptive attitude tracking on SO(3) with an application to quadrotor UAV. IEEE Trans. Control Syst. Technol. **21**(5), 1924–1930 (2013)
14. Mayhew, C., Sanfelice, R., Teel, A.: Quaternion-based hybrid control for robust global attitude tracking. IEEE Trans. Autom. Control **56**(11), 2555–2566 (2011)
15. Sarlette, A., Sepulchre, R., Leonard, N.E.: Autonomous rigid body attitude synchronization. Automatica **45**(2), 572–577 (2009)

16. Zhu, B.: Nonlinear adaptive neural network control for a model-scaled unmanned helicopter. Nonlinear Dyn. **78**(3), 1695–1708 (2014)
17. Kristic, M., Kanellakopoulos, I., Kokotovic, P.: Nonlinear and Adaptive Control Design. Wiley, New York (1995)
18. Chen, W.H.: Disturbance observer based control for nonlinear systems. IEEE/ASME Trans. Mechatron. **9**(4), 706–710 (2004)
19. Lee, T.Y.: Exponential stability of an attitude tracking control system on SO(3) for large-angle rotational maneuvers. Syst. Control Lett. **61**(1), 231–237 (2012)
20. Tee, K.P., Ge, S.S., Tay, E.H.: Barrier Lyapunov functions for the control of output-constrained nonlinear systems. Automatica **45**(4), 918–927 (2009)
21. Zhu, B.: Nonlinear control system designs for smallscale unmanned helicopter. Ph.D thesis, BUAA, Beijing, China (2013)
22. Chen, M., Ge, S.S., Ren, B.B.: Adaptive tracking control of uncertain MIMO nonlinear systems with input constraints. Automatica **47**(3), 452–465 (2011)
23. Ren, B.B., Ge, S.S., et al.: Adaptive neural control for output feedback nonlinear systems using a barrier Lyapunov function. IEEE Trans. Neural Netw. **21**(8), 1339–1345 (2010)
24. Marconi, L., Naldi, R.: Robust full degree-of-freedom tracking control of a helicopter. Automatica **43**(3), 1909–1920 (2007)
25. Isidori, A., Marconi, L., Serrani, A.: Robust nonlinear motion control of a helicopter. IEEE Trans. Autom. Control **48**(3), 413–426 (2003)
26. Kim, H., Shim, D.: A flight control system for aerial robots: algorithms and experiments. Control Eng. Pract. **11**(12), 1389–1400 (2003)
27. Raptis, I.A., Valavanic, K.P.: A novel nonlinear backstepping controller design for helicopters using the rotation matrix. IEEE Trans. Control Syst. Technol. **19**(2), 465–473 (2011)
28. Shuster, M.D.: A survey of attitude representations. J. Astronaut. Sci. **41**(4), 439–517 (1993)
29. Hu, J.C., Zhang, H.: Immersion and invariance based command-filtered adaptive backstepping control of VTOL vehicles. Automatica **49**(7), 2160–2167 (2013)
30. Guo, Y., Song, S.M.: Adaptive finite-time backstepping control for attitude tracking of spacecraft based on rotation matrix. Chin. J. Aeronaut. **27**(2), 375–382 (2014)
31. Gavrilets, V.: Autonomous aerobatic maneuvering of miniature helicopter. Ph.D thesis, MIT (2003)